Acta Neuropathol (1991) 83: 12–20

Acta Neuropathologica

Immunoreactivity of CD45, a protein phosphotyrosine phosphatase, in Alzheimer's disease*

E. Masliah, M. Mallory, L. Hansen, M. Alford, T. Albright, R. Terry, P. Shapiro, M. Sundsmo, and T. Saitoh

University of California, San Diego, School of Medicine, Department of Neurosciences, La Jolla, CA 92093-0624, USA

Received June 3, 1991/Revised, accepted July 31, 1991

Summary. Both protein kinases and phosphoprotein phosphatases are important components of signal transduction systems in cells. Recent studies in Alzheimer's disease (AD) have shown abnormal protein phosphorylation in the cortex suggesting an alteration in these enzymes. In the present study, an antibody against CD45 was used to analyze the status of this protein phosphotyrosine phosphatase in AD. We studied and quantified the immunohistochemical and immunochemical distribution of this integral membrane protein in control and AD brain. We found that anti-CD45 immunostained the great majority of microglia, both resting and activated. These cells were *Ricinus communis* agglutinin I positive and glial fibrillary acidic protein and neurofilament negative. The AD frontal cortex showed a 35 % ($P < 0.01$) increase in the number of anti-CD45 immunoreactive microglia as compared with controls. These results were consistent with the immunoblot quantification of CD45 immunoreactivity following native gel electrophoresis. In AD, 30 % of the CD45-immunostained microglia were clustered in the neuritic plaques (about six per plaque) while the remaining 70 % were scattered in the neuropil. The AD hippocampus showed an increase in CD45-immunoreactive microglia in the molecular layer of the dentate gyrus. At the ultrastructural level, CD45 immunoreactivity was localized exclusively to the plasma membrane of the microglia. The presence of the anti-CD45 immunoreactivity in microglia suggests the possibility that they may require the presence of CD45 as a cell surface receptor which may regulate cell function through modulation of intracellular signaling.

Key words: CD45 – Protein phosphotyrosine phosphatase – Microglia – Intracellular signaling – Alzheimer's disease

* Supported by National Institutes of Health grants AG08205, AG08201, and AG05131, PEW Caritable Trust, and the Alzheimer's Association/George F. Berlinger Memorial Faculty Scholar Award

Offprint requests to: E. Masliah (address see above)

One of the characteristics of Alzheimer's disease (AD) is abnormal protein phosphorylation in the cortex [6, 14, 21, 28, 33–35]. Aberrant phosphorylation has been identified in several proteins including tau [12, 40], microtubule-associated protein (MAP)5 [13], a 60-kDa protein [32] and a 86-kDa protein [6]. Although relatively extensive research has been done to study abnormal kinase activity in AD, almost no information is available about the role of phosphoprotein phosphatases in AD pathogenesis.

CD45 is a family of cell surface glycoproteins [39], found mainly in lymphocytes, with the potential to mediate signal transduction through its protein phosphotyrosine phosphatase activity [38]. In particular, the intracellular domain of CD45 has been shown to dephosphorylate $p56^{lck}$, a *src*-type protein tyrosine kinase (PTK), at the regulatory Tyr^{505} site leading to its activation [31]. In an earlier study [35], we found markedly elevated levels of two phosphotyrosine-containing proteins (55 and 60 kDa) in AD brain, as well as altered PTK activity. Previously, CD45 has been studied in the brain as a microglial marker [1, 2, 4, 15, 26, 27, 29], but not as a protein tyrosine phosphatase. We sought the possibility that CD45 may be involved in the dephosphorylation of proteins abnormally phosphorylated at the tyrosine residue in the AD brain. For the present study, we analyzed and quantified the immunohistochemical, immunochemical and ultrastructural distribution of the integral membrane protein CD45, a protein phosphotyrosine phosphatase, in the control and AD brain. In contrast to many kinases which are found enriched in neurons, CD45 was found predominantly in microglia.

Materials and methods

Samples

Twelve autopsy cases from the Alzheimer's Disease Research Center at the University of California, San Diego were utilized in

the present analysis. Seven of the cases had clinical histories of AD which was confirmed at autopsy. The average age of the AD cases was 77 ± 10 years, with a postmortem delay of 5 ± 2 h. The other five cases were clinically and histopathologically free of neurological disease. The average age of these control cases was 73 ± 12 years with a postmortem delay of 6 ± 2 h. In each of the 12 cases, blocks taken from the frontal cortex and posterior hippocampus were fixed in 2 % buffered paraformaldehyde for 72 h at 4 °C. The tissue was then serially sectioned at 40 μm with the Oxford vibratome.

Antibodies

The mouse monoclonal antibody against CD45 (Oncogene Science, Inc., Manhasset, N.Y.) was used to study the localization of protein phosphotyrosine phosphatase in the control and AD brain. The antibody was purified from mouse ascitis fluid after inoculating the clone (T29/33) obtained from BALB/c mice immunized with the human T leukemic cell line CCR-CEM. The antibody characteristics and specificity are described elsewhere [3, 30]. The lectin *Ricinus communis* agglutinin I (RCA-I, Vector Laboratories, Inc., Burlingame, Calif.) was used to identify microglia in the human brain [19]. Astrocytes were identified with a rabbit polyclonal antibody against glial fibrillary acidic protein (GFAP) (Sigma Chemical Co., St. Louis, Mo.), and neuritic processes were labeled with the rabbit polyclonal antibody against neurofilament 200 (Sigma).

Immunohistochemistry

The vibratome sections were first washed in phosphate-buffered saline (PBS) (pH 7.4), blocked with 10 % normal horse serum, and incubated overnight at 4 °C with anti-CD45 (mouse monoclonal antibody, 1:10). The free-floating sections were then washed and incubated with secondary biotinylated antibody, followed by avidin D-HRP (ABC Elite, Vector Laboratories) and reacted with diaminobenzidine (DAB; 0.2 mg/ml) in 50 mM Tris buffer (pH 7.4) with 0.001 % hydrogen peroxide. Additional frontal cortex and hippocampal sections, immunostained with anti-CD45, were counterstained with thioflavine-S. Control experiments were done by incubating sections from the age-matched control group and from the AD group with the purified mouse IgG1 ascitis (Chemicon International, Inc., Los Angeles, Calif.; 1 μg/ml). This IgG1 is a good control for the CD45 antibody since they both are obtained from mouse-mouse hybrid cells, are both ascitis and are of the same immunoglobulin class.

Morphometry

Anti-CD45-immunostained cells were counted in ten consecutive fields (0.1 mm^2 each) along the side of the gyrus using a 40 × objective and a gridded 10 × eyepiece lens. Differential plaque counts were done in anti-CD45 immunoreacted/thioflavine-S-counterstained sections. The different plaque types were assigned to one of the three categories (diffuse, immature, and mature) according to the criteria previously described [20, 44].

Double immunolabeling and confocal laser imaging

To assess the colocalization of positive CD45 cells with RCA-I labeled microglia, 40-μm vibratome sections from control and AD cortex were double-immunolabeled [23] with anti-CD45 and biotinylated RCA-I. Sections were then incubated in a mixture of FITC-conjugated horse anti-mouse IgG (1:75) and Avidin D Texas red (1:100) (Vector Laboratories). Additional sections were double-immunolabeled with a mixture of: (a) polyclonal anti-neurofilament antibody and monoclonal anti-CD45, or (b) polyclonal anti-GFAP and monoclonal anti-CD45. The double-labeled sections were transferred to gelatin-coated slides and mounted under glass coverslips with antifading media containing 4 % *n*-propyl gallate (Sigma). The sections were studied with the Bio-Rad MRC-600 laser scanning microscopy [20] mounted on an Axiovert Zeiss microscope. This system permits the simultaneous analysis of double-immunolabeled samples in the same optical plane.

Images of 0.5-μm-thick optical sections of the neocortical neuropil displaying the anti-CD45-immunolabeled cells were recorded as well as the corresponding serial images of the RCA-I, anti-neurofilament or anti-GFAP-immunolabeled cells. The digitized video images were stored on an optical disk for subsequent display, analysis and quantification. The aperture, black, and gain level were initially adjusted manually to obtain images with a pixel intensity within a linear range. In all sections the images were acquired while maintaining the above-described parameters constant [20].

Immunoelectron microscopy

Briefly, as previously described [24] the vibratome sections were washed in PBS (pH 7.4), blocked with 10 % normal goat serum, and incubated overnight at 4 °C with anti-CD45 (1:10). The free-floating sections were then washed and incubated with biotinylated secondary antibody, followed by avidin D-HRP (ABC Elite, Vector Laboratories) and reacted with DAB (0.2 mg/ml) in 50 mM Tris buffer (pH 7.4) with 0.001 % hydrogen peroxide. To prevent the artifactual diffusion of the chromogen, the sections were incubated in 1 % glutaraldehyde in 0.15 M cacodylate buffer [45] before the DAB reaction. Control experiments were done by incubating sections from the age-matched control group and from the AD group with purified mouse IgG1 ascitis (Chemicon International, Inc., 1 μg/ml). The immunostained sections were postfixed for 20 min in 1 % osmium tetroxide in 0.15 M cacodylate buffer, dehydrated in graded alcohols, and flat-embedded in epoxy/Araldite. The sections were than placed on slides and explored with the light microscope for relevant areas displaying immunolabeled cells. These areas were trimmed and re-embedded in epoxy and polymerized at 60 °C for 48 h. Ultrathin sections were cut with a Reichert OM-U3 ultramicrotome and viewed with a 100 CX JEOL electron microscope.

Immunochemical analysis

AD and control human midfrontal cortex particulate fractions were prepared as described by Saitoh and Dobkins [32]. Protein concentrations were determined by the method of Lowry et al. [18]. Forty micrograms of protein in native gel sample buffer containing 4 % glycerol, 62 mM Tris-HCl (pH 6.8), 5 mM EDTA, 0.02 % bromophenol blue, and 0.1 % Triton X-100 was loaded onto a 5 %–10 % polyacrylamide native gel containing 0.1 % Triton X-100 and 0.38 M Tris-HCl (pH 8.8). The samples were electrophoresed until the bromophenol blue dye front was 1 cm from the end of the gel. The proteins were electroblotted onto nitrocellulose at 300 mA for 4 h in 10 mM CAPS (pH 10.5) containing 20 % methanol. The blot was then treated as follows: (1) blocked for 1 h at room temperature in 0.1 % Tween-20 PBS (TPBS); (2) incubated overnight at 4 °C with anti-CD45; (3) washed three times for 5 min at 4 °C with TPBS; (4) incubated for 2 h at 4 °C with rabbit anti-mouse IgG (H + L) Accurate Chemical Corp., Westbury, N.Y.) diluted 1:2000 in 3 % BSA/PBS; (5) washed three times for 5 min with TPBS; (6) incubated for 2 h at 4 °C with 0.5 μCi/ml ^{125}I-labeled Protein A (>30 μCi/μg; ICN, Irvine, Calif.), 7) rapidly washed five times with TPBS and exposed to RP-X-omat X-ray film at –80 °C with intensifying screens for 15 h. The intensity of the CD45-

immunopositive band was quantified using a laser scanning densitometer (LKB Ultrascan, Pharmacia, Uppsala, Sweden).

Results

Anti-CD45 immunolocalization in the neocortex

Anti-CD45 immunostained a population of cells characterized by small oval nuclei with fine, abundant, and ramified processes (Fig. 1). Laser confocal imaging of double-immunolabeled sections showed that the anti-CD45-immunostained cells were RCA-I positive (Fig. 2), but were anti-GFAP and anti-neurofilament negative. These cells were identical to microglia. The computer-assisted image analysis showed that the CD45-immunostained microglia had an average area of 160 μm^2, their average perikaryon measured 18 μm in length and 4 μm in width, and their processes were 16 to 23 μm in length. Anti-CD45 immunostained a greater proportion of microglia as compared to RCA-I. In addition, while RCA-I labeled blood vessels, anti-CD45 did not. The control neocortex presented a homogeneous distribution of these cells throughout the layers. In these samples the anti-CD45 immunostained microglia presented fine, elongated processes without any microglial clustering. Anti-CD45 did not stain neurons or astrocytes in the control cases. The white matter showed a higher density of microglia per square micrometer than gray matter. In the white matter the immunoreactive microglia were smaller and were distributed along the myelinated fibers (Fig. 1C, D).

The AD neocortex presented a 35% increase ($P < 0.01$) (Fig. 3) in the density of anti-CD45-immunostained scattered microglia as compared to controls. The immunolabeled microglia were swollen and had long, distended processes. Layers 1 and 2 of the AD neocortex (Fig. 4A–C) showed a stronger anti-CD45 immunoreactivity probably due to an increase in the number of microglial processes. To asses the concentration of CD45 biochemically, we first immunostained a nitrocellulose blot (Western blot) of particulate proteins separated on a SDS-polyacrylamide gel. Anti-CD45, however, did not detect any bands. Since dot blot analysis confirmed that the reducing/denaturing conditions destroyed CD45 immunoreactivity (not shown), we separated the proteins on a native polyacrylamide gel followed by Western blotting. Anti-CD45 stained a single band on the native gel when the AD and control samples were analyzed (Fig. 5A). The intensity of the anti-CD45-immunoreactive band, as quantified by laser scanning densitometry, revealed that the amount of this band in AD samples was significantly elevated as compared to controls ($P < 0.05$ by ANOVA) (Fig. 5B).

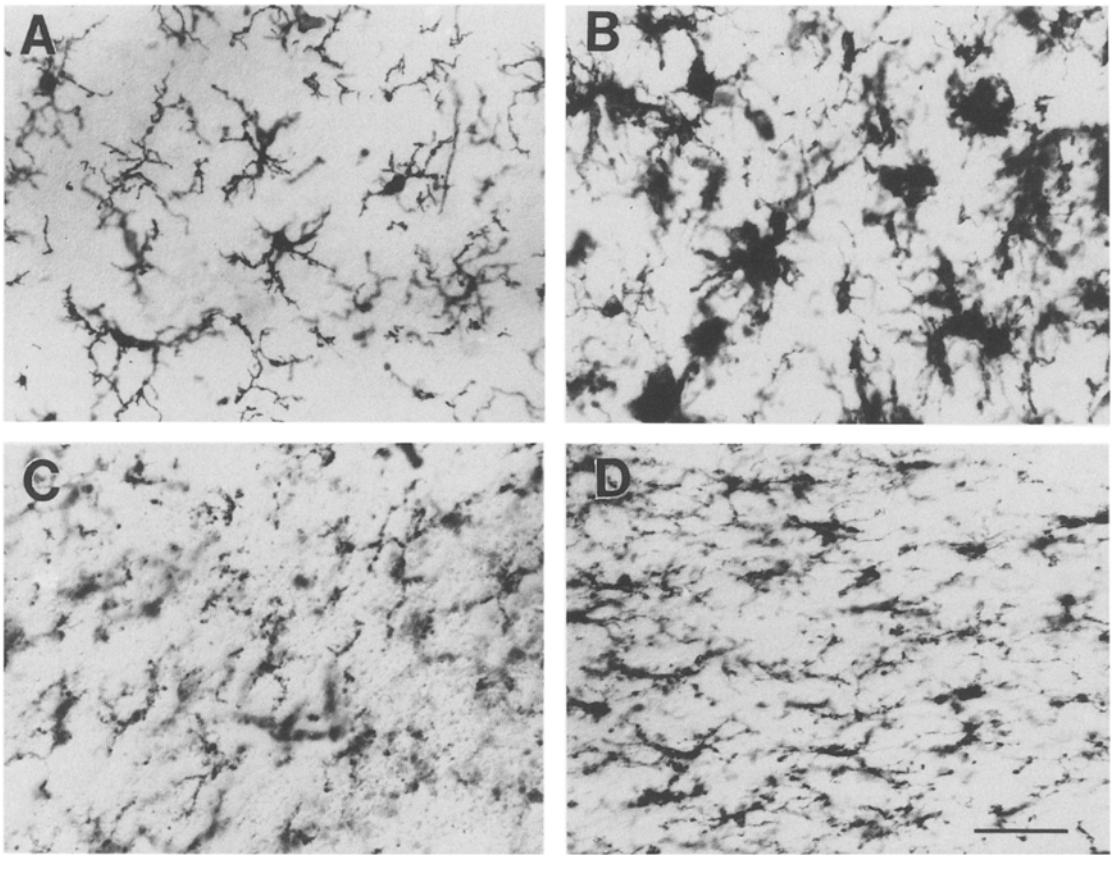

Fig. 1A–D. CD45 immunoreactivity in the human neocortex. **A** Layer 3 of the control frontal cortex showed ramified anti-CD45-immunostained microglia. **B** Layer 3 of the Alzheimer's disease (AD) frontal cortex showed abundant activated anti-CD45-stained microglia. **C** The control white matter presented some small, ramified microglia. **D** in AD, there was a relative increase in the CD45-immunoreactive microglia in the white matter. Bar = 20 μm

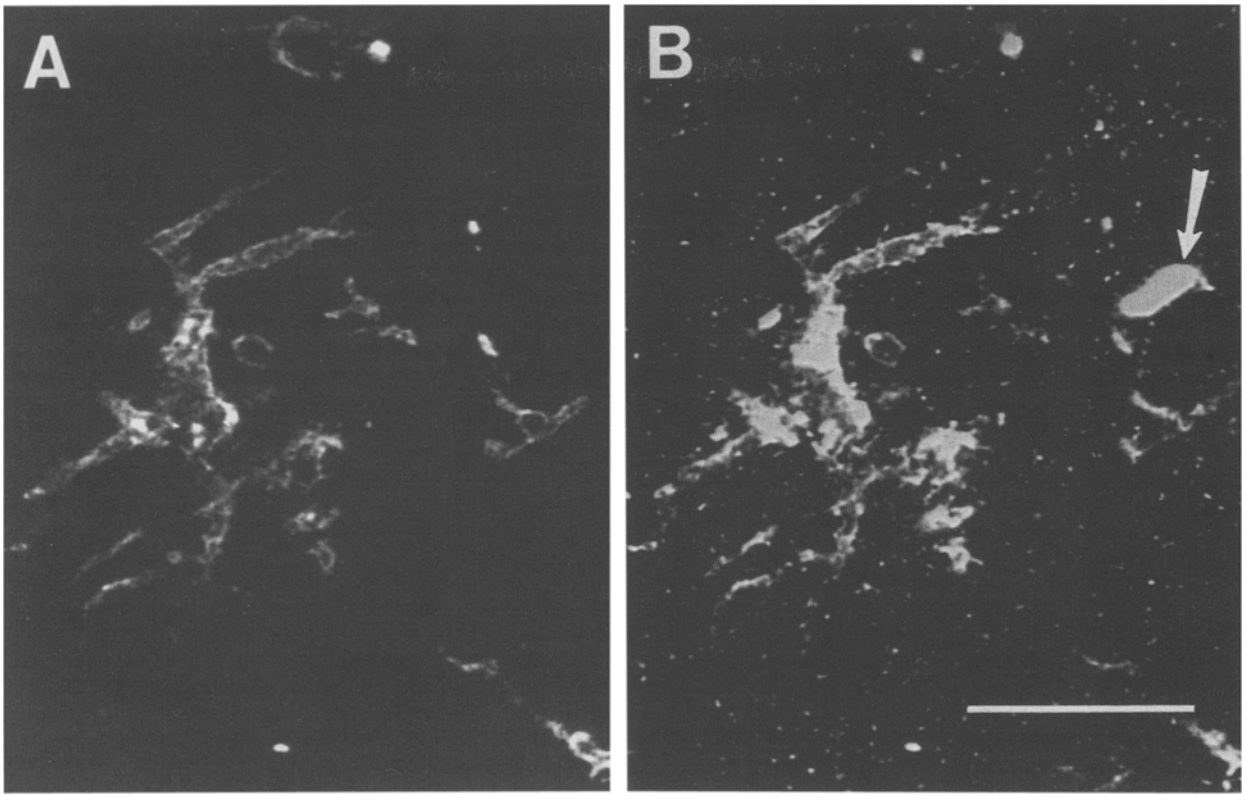

Fig. 2A, B. Laser confocal imaging of the double-immunolabeled sections for CD45-FITC (**A**) and RCA I-Texas red (**B**). **A** CD45-immunoreactive microglia were colocalized with **B:** Ricinus communis agglutinin-1 (RCA-I)-positive microglia. *Arrow* indicates autofluorescent lipofuscin. Bar = 15 μm

A prominent feature in the AD cases was the clustering of microglia in the plaques, mostly in layers 3 and 5 (Fig. 4D–F). The thioflavine-S-counterstained sections showed that on the average, approximately 60% of the total number of plaques were diffuse plaques, the other 40% were immature and mature plaques. Diffuse plaques lacked at CD45-positive microglial component, while in contrast the great majority of the immature and mature plaques contained anti-CD45-immunoreactive microglial clusters. In these regions, the immunoreactive microglia were extremely swollen and displayed long intermingled processes with focal dilatations. The computer-assisted image analysis showed that these CD45-immunolabeled microglia clusters had an average of 567 μm^2, and an average diameter of 30 μm. The microglia clusters were composed of an average of six cells per neuritic plaque. Of the total immunostained microglia, 30% were located in the

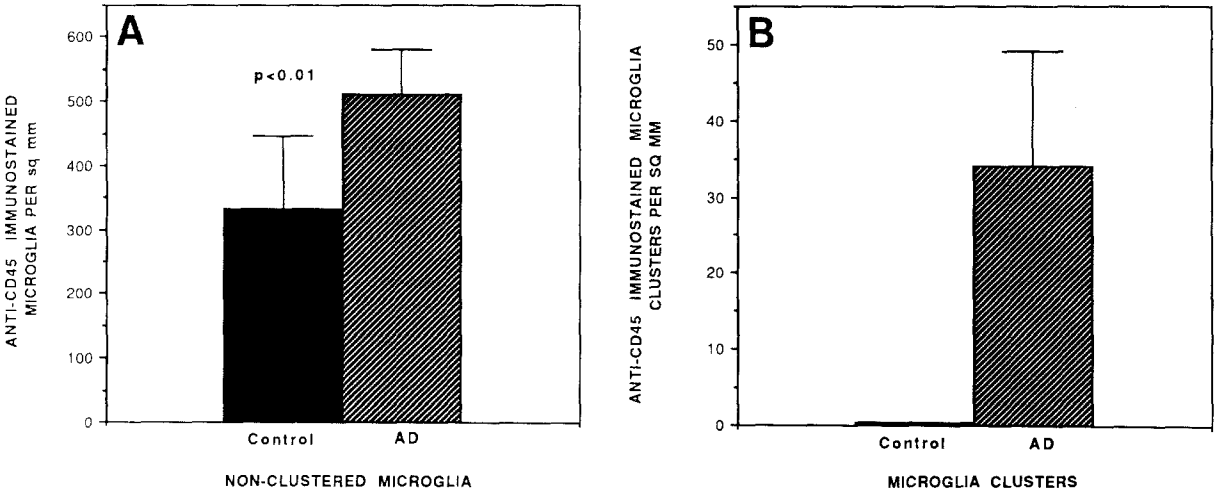

Fig. 3A, B. Quantification of anti-CD45-immunostained microglia in the frontal cortex. **A** in AD, there was a 35% increase in the CD45-immunoreactive, non-clustered microglia. **B** The AD samples presented an average of 33 microglia clusters/mm^2 composed of, on average, 6 microglia per cluster. No clusters were found in the controls. Bars are SD. n = 4 control and 6 AD cases

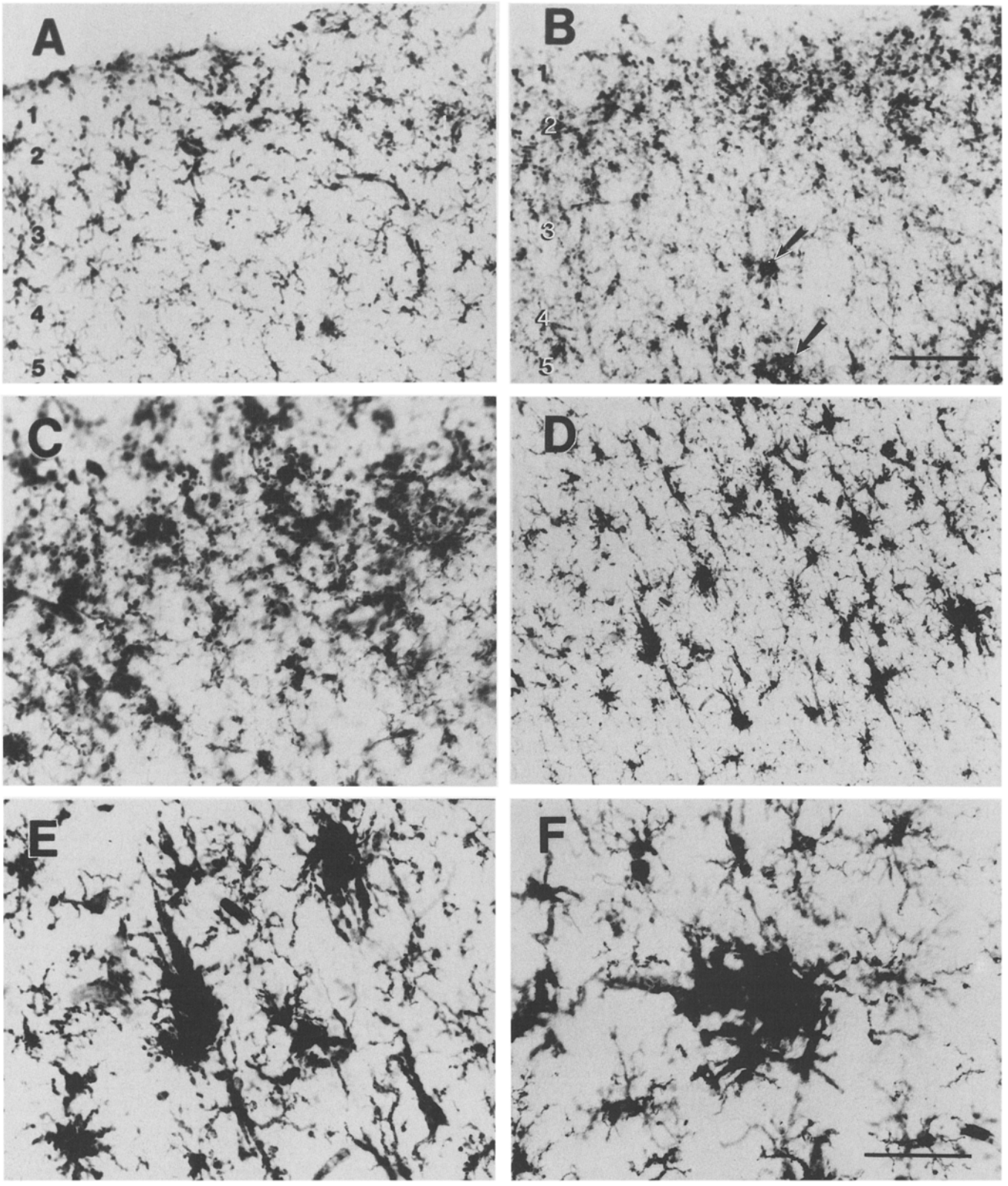

Fig. 4A–E. Patterns of CD45-immunostained microglia in the control and AD neocortex. **A** The control cortex showed an homogeneous distribution of ramified microglia throughout the layers of the cortex. **B** In AD, there was an increase in CD45-immunoreactive swollen microglial processes in layer 2, with microglial clusters (*arrows*) in layers 3 and 5. **C** Higher magnification of the swollen microglial processes in layer 2. **D** Additionally, in AD, anti-CD45 immunostained large microglia with elongated processes. **E** Higher magnification of D. **F** Higher magnification of a microglial cluster. Bars **A, B, D** = 40; **C, E, F** = 20 μm

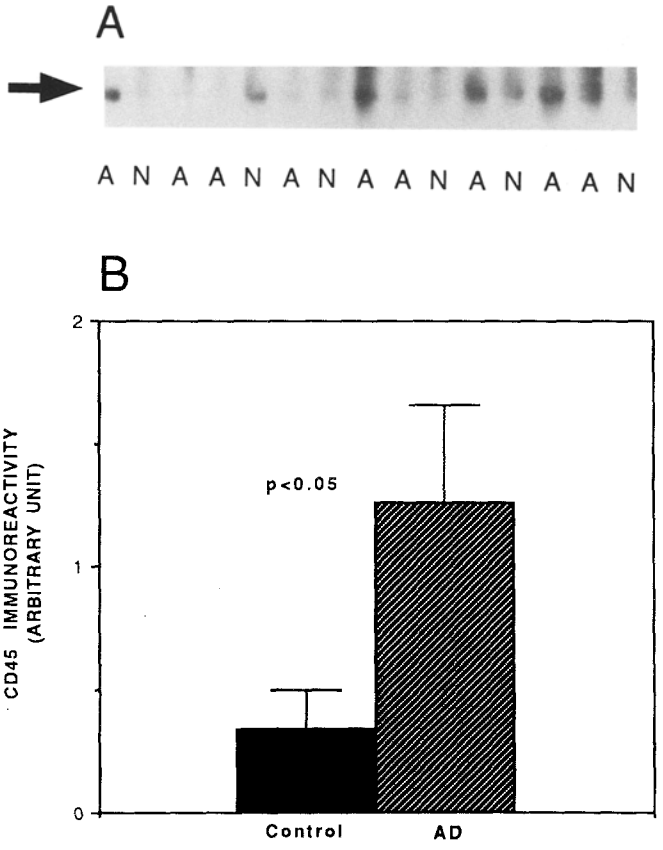

neuritic plaques as microglial clusters and the remaining 70 % were scattered in the neuropil. Only few pyramidal neurons were slightly immunolabeled by anti-CD45 in AD. The AD white matter showed abundant, small, immunolabeled microglia, some of them swollen (Fig. 1D). Only a few microglia clusters were noted in the white matter.

At the ultrastructural level, anti-CD45-immunostained microglia showed a strong immunoreactivity in the plasma membrane of the cell body, as well as in the cellular processes (Fig. 6). No immunostaining was found in the endomembranous system, in the nuclear membrane or in the other membranous organelles. In the control experiments, where sections were immunoreacted with purified IgG1 ascitis, the microglial plasma membrane did not react.

Fig. 5A, B. Western blot analysis of CD45. **A** Particulate fractions prepared from control and AD frontal cortex are separated on a native gel containing Triton X-100, electroblotted, and immunostained with anti-CD45 antibody. Only one band was detected on the blot by this antibody. *A* denotes AD and *N* denotes normal specimens. **B** To asses the concentration of CD45 in each sample, the intensity of the anti-CD45-positive bands on the Western blot was quantified and averaged for the two groups. The mean intensity of anti-CD45 bands in AD cortex is significantly larger than the control ($P < 0.05$ by ANOVA). Bars are SEM. $n = 6$ controls and 9 AD cases

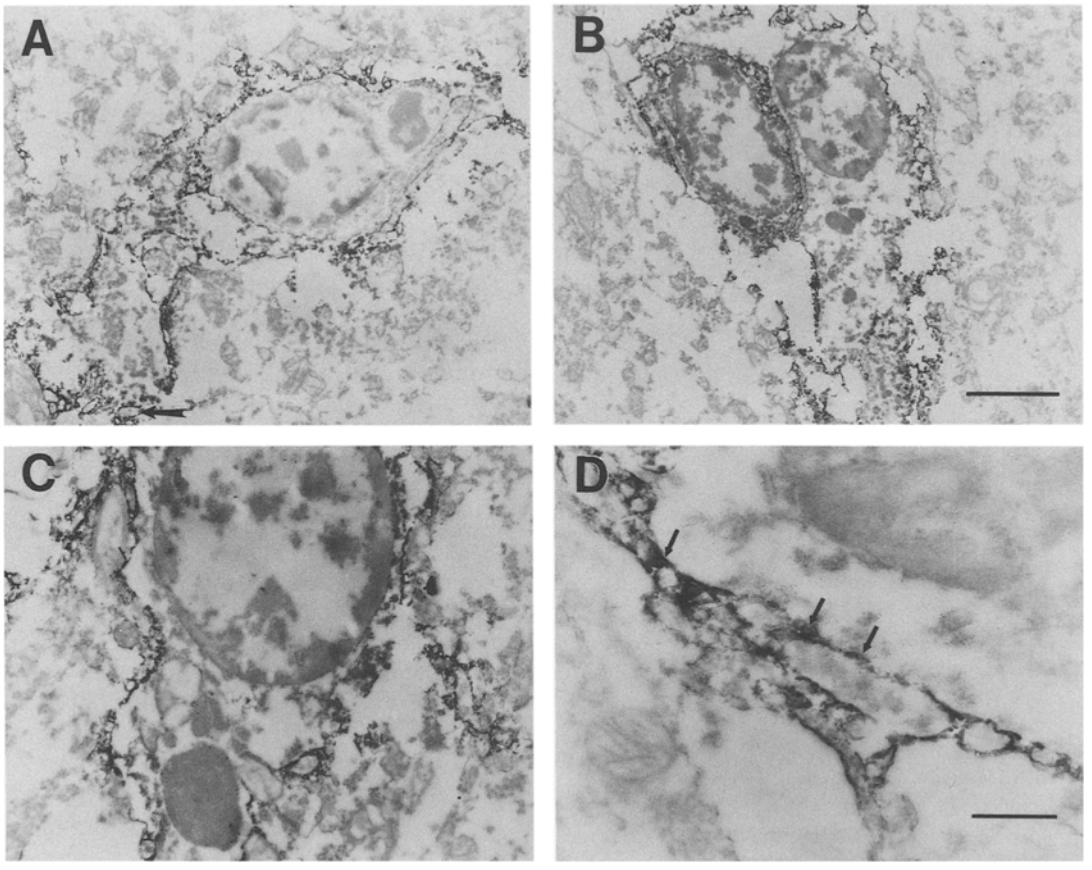

Fig. 6A–D. Immunoelectron microscopy of CD45. **A** Lower magnification of a microglia in AD immunostained with anti-CD45. Plasma membranes of the cell body and cellular processes were immunolabeled. **B** CD45-immunostained microglial cluster. **C** The reaction products is exclusively located in the plasma membrane, but not in the nuclear membrane. **D** Higher magnification of the immunostained plasma membrane; no staining is observed in the intracellular organelles. Bars **A, B** = 3; **C, D** = 1 μm

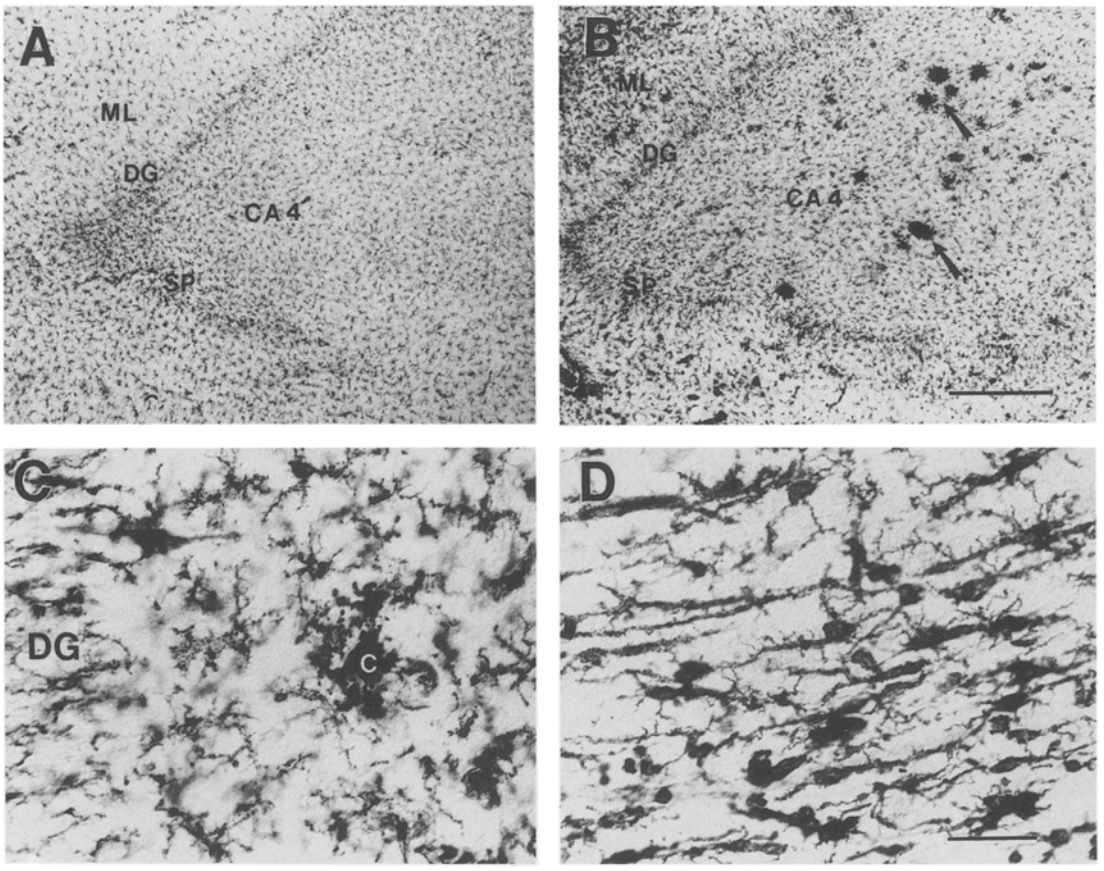

Fig. 7A–D. CD45 immunoreactivity in the hippocampus. **A** The control hippocampus showed strong microglial immunoreactivity throughout the layers with higher density in the stratus polymorphous (*SP*) and CA4 regions. *DG:* Dentate gyrus; ML molecular layer. **B** In AD, there was an increased immunostaining in the molecular layer and in the CA4 region (*arrows*). **C** Higher magnification of the AD molecular layer which showed a microglial cluster (*C*). **D** The microglia in the pyramidal layer region of the AD cases were elongated and rod shaped. Bars A, B = 100; C, D = 20 μm

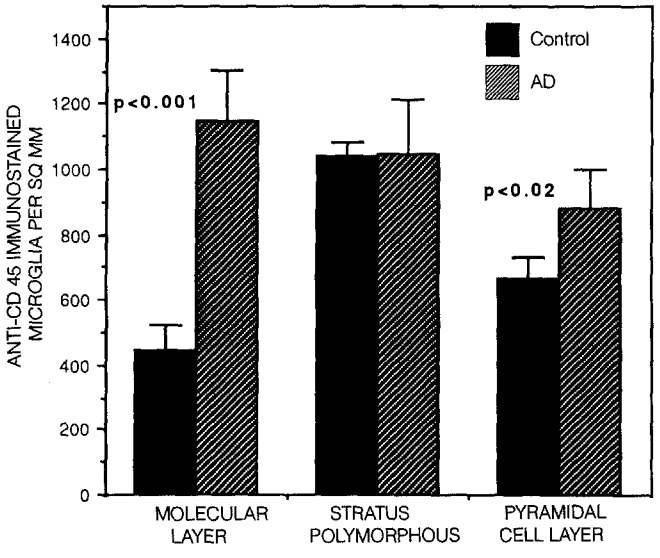

Fig. 8. Quantification of anti-CD45-immunostained microglia in the hippocampus. The AD cases presented a significant increase in microglial density in the molecular layer and in the pyramidal cell layer. No significant differences were found between the control and AD cases in the stratus polymorphous. Bars are SD. $n = 4$ control and 6 AD cases

Anti-CD45 immunolocalization in the hippocampus

The control hippocampus (Fig. 7A) showed abundant, small, CD45-immunoreactive microglia mostly concentrated in the stratus polymorphous and in the cornus ammonis. The AD hippocampus (Fig. 7B) presented a greater microglial density in the molecular layer (Figs. 7C, 8). In contrast, the microglial density in the stratus polymorphous was not altered in AD as compared to control (Fig. 8) Anti-CD45-immunoreactive microglial clusters were concentrated in CA3 and CA2 regions of the AD hippocampus. In the pyramidal cell layer of the AD hippocampus, the microglia had long processes that were lined up with the perikarya and cell processes of the neurons (Fig. 7D). This microglial pattern was not seen in the control hippocampus. The microglial density was significantly increased in this region (Fig. 8).

Discussion

CD45 [39] is a family of high-molecular-weight surface proteins expressed in cells of hematopoietic lineage also

referred to as leukocyte common antigen [37], T200 [30], B220 [85], and Ly-5 [16]. Six isoforms of CD45 have been described with molecular masses of 180 to 220 kDa [39]. CD45 is a cell surface glycoprotein with the potential to regulate signal transduction through the protein phosphotyrosine dephosphorylation route. Consistent with previous studies [26, 29], our immunohistochemical analysis showed that the monoclonal antibody against CD45 immunostained the microglial cell population in the control and AD cortex. This antibody recognizes all members of the CD45 family and is considered to be a marker of cells of hematopoietic origin [37]. Anti-CD45 has been previously used in differentiating non-Hodgkin's lymphoma from non-hematopoietic neoplasms [3] as well as in the assessment of the macrophage infiltration in gliomas [29]. Previous studies have suggested that microglia may have originated from pial, pericytic, monocytic, glial ectodermal cells or a combination of any of the above [8]. The presence of the anti-CD45 immunoreactivity in microglia supports the possibility that these cells are derived from the monocyte/macrophage lineage or from its hematopoietic precursor. It also suggests that microglia may require the presence of CD45 as a cell surface receptor which may regulate cell function by transmembrane signal transduction [38].

Consistent with the proposed characterization of CD45 as a cell surface receptor [37, 39], our immunoelectron microscopic study revealed that anti-CD45 immunoreactivity was restricted to the plasma membrane of the microglia. CD45 phosphotyrosine phosphatase activity is in the cytoplasmic domain and it has been shown in vitro to dephosphorylate myelin basic protein, as well as autophosphorylated preparations of epidermal growth factor receptor, insulin receptor, and $p56^{lck}$ protein tyrosine kinases [39].

Anti-CD45 antibody recognized both resting and activated microglia [1, 2, 4, 15, 26, 27, 29]. In AD it immunostained activated microglia clustered in the neuritic plaques, as well as those scattered in the neuropil. Wisniewski and his colleagues [41, 42] proposed, based on ultrastructural studies, that the microglia in the neuritic plaque could be either phagocytizing or synthesizing the amyloid fibers. In this regard, CD45 could be involved in intracellular signaling required for these cellular functions in the clustered microglia via intracellular phosphotyrosine phosphatase activity. It is, however, unlikely that CD45 is involved in the dephosphorylation of amyloid β/A4 protein precursor (APP) derived from the microglia [7], because in vitro studies have shown that phosphorylation of APP is on serine-655 by PKC or on threonine-654 by Ca^{2+}/calmodulin-dependent kinase II [10]. Furthermore, the APP fragment (645–661) was an ineffective substrate for insulin-dependent protein tyrosine kinase [10]. Additionally, Wood and Zinsmeister [43] showed phosphotyrosine immunoreactivity in the tangle-bearing neurons, the dystrophic neurites, and probably in the microglia in the plaque suggesting that tyrosine phosphorylation might be involved in the microglial response in AD pathology.

We also found an increase in the number of anti-CD45-immunoreactive microglia scattered in the AD neuropil, which was consistent with the increase in the anti-CD-45-immunoreactive band in the native gel. Microglia could be involved in the process of antigen presentation and processing [36]. In this regard, CD45 may work as a cell surface receptor for an as yet unidentified ligand initiating a signal transduction mechanism resulting in microglial activation. Alternatively, it could be involved in the process of neuropil remodeling, possibly through the production of lymphokines such as interleukin-I [9, 11]. Microglia have been shown to appear after Wallerian degeneration [17]. The increase in the number of CD45-immunoreactive microglia was in layers 2, 3, and 5 of the neocortex and molecular layer of the hippocampus, areas in which previous studies have shown extensive synaptic damage [22] and remodeling [25].

Since most of the tyrosine phosphatase-CD45 immunoreactivity was localized to the microglia, it is unlikely that this particular phosphatase will have a direct role in processing the abnormally phosphorylated proteins present in the AD neurons. Furthermore, the up-regulation of CD45 in microglia has been reported in multiple sclerosis [4], and in kainic acid-lesioned brain [2]. Future studies are necessary to identify the ligand for CD45 and its role in AD pathogenesis as well as to identify other protein tyrosine phosphatases present in the AD neurons.

Acknowledgements. The authors wish to thank Robert Davignion for editing the manuscript.

References

1. Akiyama H, McGeer PL (1990) Brain microglia constitutively express β-2 integrins. J Neuroimmunol 30:81–93
2. Akiyama H, Itagaki S, McGeer PL (1988) Major histocompatibility complex antigen expression or rat microglia following epidural kainic acid lesions. J Neurosci Res 20:147–157
3. Battifora H, Trowbridge IS (1983) A monoclonal antibody useful for the differential diagnosis between malignant lymphoma and nonhematopoietic neoplasms. Cancer 51:816–821
4. Boyle EA, McGeer PL (1990) Cellular immune response in multiple sclerosis plaques. Am J Pathol 137:575–584
5. Coffman RL, Weissman IL (1981) B220: a B cell-specific member of the T200 glycoprotein family. Nature 289:681–683
6. Cole G, Dobkins KR, Hansen LA, Terry RD, Saitoh T (1988) Decreased levels of protein kinase C in Alzheimer brain. Brain Res 452:165–170
7. Currie J, Barcikowska M, Wegiel J, Morys J, Wisniewski HM (1989) Antiserum raised against a subsequence of Alzheimer amyloid precursor protein selectively labels a subset of microglial cells. J Neuropathol Exp Neurol 48:328
8. Dolman CL (1985) Microglia. In: Davis RL, Robertson DM (eds) Textbook of neuropathology. Williams & Wilkins, Baltimore, pp 117–137
9. Fagan AM, Gage FH (1990) Cholinergic sprouting in the hippocampus: a proposed role for IL-1. Exp Neurol 110:105–120

10. Gandy S, Czernik AN, Greengard P (1988) Phosphorylation of Alzheimer disease amyloid precursor peptide by protein kinase C and Ca^{++}/calmodulin-dependent protein kinase II. Proc Natl Acad Sci USA 85:6218–6621
11. Griffin WST, Stanley LC, Ling C, White L, Mac Leod V, Perrot LJ, White CL, Araoz C (1989) Brain interleukin 1 and S-100 immunoreactivity are elevated in Down syndrome and Alzheimer disease. Proc Natl Acad Sci USA 86:7611–7615
12. Grundke-Iqbal I, Iqbal K, Tung Y-C, Quinlan M, Wisniewski HM, Binder LI (1986) Abnormal phosphorylation of the microtubule-associated protein tau in Alzheimer cytoskeletal pathology. Proc Natl Acad Sci USA 83:4913–4917
13. Hasegawa M, Arai T, Ihara Y (1990) Immunochemical evidence that fragments of phosphorylated MAP5 (MAP1B) are bound to neurofibrillary tangles in Alzheimer's disease. Neuron 4:909–918
14. Iimoto DS, Masliah E, De Teresa R, Terry RD, Saitoh T (1990) Aberrant casein kinase II in Alzheimer's disease. Brain Res 507:273–280
15. Itagaki S, McGeer PL, Akiyama H (1988) Presence of T-cytotoxic suppressor and leukocyte common antigen positive cells in Alzheimer's disease brain tissue. Neurosci Lett 91:259–264
16. Komuro K, Itakura K, Boyse EA, John M (1975) Ly-5: a new T-lymphocyte antigen system. Immunogenetics 1:452–456
17. Ling EA (1979) Evidence for a hematogeneous origin of some of the macrophages appearing in the spinal cord of the rat after dorsal rhizotomy. J Anat 128:143–154
18. Lowry OH, Rosebrough NJ, Farr AL, Randall RJ (1951) Protein measurement with Folin phenol reagent. Biol Chem 193:265–272
19. Mammoji H, Yeger H, Becker LE (1986) A specific histochemical marker (lectin *Rhinus communis* agglutinin-1) for normal human microglia, and application to routine histopathology. Acta Neuropathol (Berl) 71:341–343
20. Masliah E, Terry RD, Mallory M, Alford M, Hansen L (1990) Diffuse plaques to not accentuate synapse loss in Alzheimer disease. Am J Pathol 137:1293–1297
21. Masliah E, Cole G, Shimohama S, Hansen LA, DeTeresa R, Terry RD, Saitoh T (1990) Differential involvement of protein kinase C isozymes in Alzheimer's disease. J Neurosci 10:2113–2124
22. Masliah E, Terry RD, Alford M, DeTeresa R, Hansen LA (1991) Cortical and subcortical patterns of synaptophysin-like immunoreactivity in Alzheimer disease. Am J Pathol 138:235–246
23. Masliah E, Yoshida K, Shimohama S, Gage FH, Saitoh T (1991) Differential expression of protein kinase C isozymes in rat primary glial cell cultures. Brain Res 549:106–111
24. Masliah E, Hansen L, Albright T, Mallory M, Terry RD (1991) Immunoelectron microscopic study of synaptic pathology in Alzheimer disease. Acta Neuropathol 81:428–433
25. Masliah E, Mallory M, Hansen L, Alford M, Albright T, DeTeresa R, Terry RD, Baudier J, Saitoh T (1991) Patterns of aberrant sprouting in Alzheimer disease. Neuron 6:729–739
26. Mattiace LA, Davies P, Dickson DW (1990) Detection of HLA-DR on microglia in the human brain is a function of both clinical and technical factors. Am J Pathol 136:1101–1114
27. McGeer PL, Akiyama H, Itagaki S, McGeer EG (1989) Immune system response in Alzheimer's disease. Can J Neurol Sci 16:516–527
28. McKee AC, Kosik KS, Kennedy MB, Kowall NW (1990) Hippocampal neurons predisposed to neurofibrillary tangle formation are enriched in type II calcium/calmodulin dependent protein kinase. J Neuropathol Exp Neurol 49:49–63
29. Morimura T, Neuchrist C, Kitz K, Budka H, Scheiner O, Kraft D, Lassmann H (1990) Monocyte subpopulations in human gliomas: expression of Fc and complement receptors and correlation with tumor proliferation. Acta Neuropathol 80:287–294
30. Omary MB, Trowbridge IS, Battifora HA (1980) Human homologue of murine T200 glycoprotein. J Exp Med 152:842–852
31. Ostergaard HL, Shackelford DA, Hurley TR, Johnson P, Hyman R, Sefton BM, Trowbridge IS (1989) Expression of CD 45 alters phosphorylation of the *lck*-encoded tyrosine protein kinase in murine lymphoma T-cell line. Proc Natl Acad Sci USA 85:8959–8963
32. Saitoh T, Dobkins KR (1986) Increased in vitro phosphorylation of a M_r 60,000 protein in brain from patients with Alzheimer disease. Proc Natl Acad Sci USA 83:9764–9767
33. Saitoh T, Iimoto DS (1989) Aberrant protein phosphorylation in Alzheimer's disease. Prog Clin Biol Res 317:769–780
34. Saitoh T, Masliah E, Jin L-W, Cole GM, Wieloch T, Shapiro IP (1991) Protein kinases and phosphorylation in neurologic disorders and cell death. Lab Invest 64:596–616
35. Shapiro IP, Masliah E, Saitoh T (1991) Altered protein tyrosine phosphorylation in Alzheimer's disease. J Neurochem 56:1152–1162
36. Streit WJ, Graber MB, Kreutzberg GW (1988) Functional plasticity of microglia: a review. Glia 1:301–307
37. Thomas ML (1989) The leukocyte common antigen family. Annu Rev Immunol 7:339–369
38. Tonks NK, Charbonneau H (1989) Protein tyrosine dephosphorylation and signal transduction. Trends Biochem Sci 14:497–500
39. Tonks NK, Diltz CD, Fischer EH (1990) CD 45, an integral membrane protein tyrosine phosphatase. Characterization of enzyme activity. J Biol Chem 265:10674–10680
40. Ueda K, Masliah E, Saitoh T, Bakalis SL, Scoble H, Kosik KS (1990) Alz-50 recognizes a phosphorylated epitope of tau protein. J Neurosci 10:3295–3304
41. Wisniewski H, Terry RD (1973) Reexamination of the pathogenesis of the senile plaques. Prog Neuropathol 2:1–26
42. Wisniewski HM, Wegiel J, Wang KC, Kujawa M, Lach B (1989) Ultrastructural studies of the cells forming amyloid fibers in classical plaques. Can J Neurol Sci 16:535–542
43. Wood JG, Zinsmeister P (1991) Tyrosine phosphorylation systems in Alzheimer's disease pathology. Neurosci Lett 121:12–16
44. Yamaguchi H, Hirai S, Morimatso M, Shoji M, Ihara Y (1988) A variety of cerebral amyloid deposits in the brains of the Alzheimer-type dementia demonstrated by β-protein immunostaining. Acta Neuropathol 76:541–549
45. Yamaguchi H, Nakazato Y, Hirai S, Shoji M (1990) Immunoelectron microscopic localization of amyloid beta protein in the diffuse plaques of Alzheimer-type dementia. Brain Res 508:320–324